

# Novel push–pull dendrons with high excited state dipole moments. Synthesis and theoretical analysis of unusual “branched electron distribution”



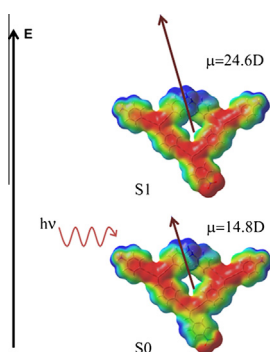
Patricia Guadarrama\*, Gerardo Terán, Estrella Ramos, Jorge Gutiérrez, Madelyn Hernández

*Instituto de Investigaciones en Materiales, Universidad Nacional Autónoma de México, Apartado Postal 70-360, CU, Coyoacán, México DF 04510, Mexico*

## HIGHLIGHTS

- Novel push–pull dendrons with high excited state dipole moments were synthesized.
- The rigidity and high delocalization of dendrons promote charge transfer mechanisms.
- Delocalized push–pull dendron (8) exhibits an unusual branched electron distribution.
- High excited state dipole moments can be related to efficient photovoltaic processes.
- Solvatochromic method is a useful tool to estimate dipole moments in excited state.

## GRAPHICAL ABSTRACT



## ARTICLE INFO

### Article history:

Received 28 August 2014  
 Received in revised form 11 December 2014  
 Accepted 11 December 2014  
 Available online 27 December 2014

### Keywords:

Push–pull  
 Dendron  
 Solvatochromic method  
 Excited state dipole moments  
 DFT

## ABSTRACT

The synthesis of novel highly delocalized push–pull dendrons is described. A modified protocol to conventional C–C coupling reaction was used with moderate yields. The excited state dipole moments of synthesized dendrons were estimated by the solvatochromic model using the  $E_N^R$  polarity scale. In case of dendron of second generation with donor–acceptor groups, values around 23 D are obtained, denoting an efficient charge separation crucial in photovoltaic processes. From the theoretical analysis, there is a clear evidence of highly efficient electron delocalization in case of push–pull dendrons. The chosen theoretical model (M05-2X/cc-pVDZ) to describe the electronic behavior of the molecules under study was very precise in the estimation of dipole moments in excited state, with differences of 0.5–2.2 D, compared with the values obtained by the solvatochromic model.

© 2014 Elsevier B.V. All rights reserved.

## Introduction

In the area of materials science, efforts have been made to propose new materials able to mediate the conversion of energy from sunlight to be used in optoelectronic devices such as solar cells, extensively developed during the past 30 years. Organic materials

have found wide acceptance in this field due to their low cost, flexibility and easy processing. The molecular systems known as push–pull or excitonic materials are promising as organic photovoltaics (OPVs) [1–3], and have been explored in different molecular architectures, including the non-conventional highly branched dendritic framework [4], resulting in potential organic materials for efficient photogeneration and separation of charges [5–8]. Previously in our group were theoretically studied a set of dendritic molecules (and their linear counterparts), demonstrating that

\* Corresponding author.

E-mail address: [patriciagua@iim.unam.mx](mailto:patriciagua@iim.unam.mx) (P. Guadarrama).

dendritic architecture of push-pull molecules favors the charge transfer in the excited state compared to linear molecules [9]. The dissociation of photogenerated electron–hole pairs (excitons) into free charge carriers is crucial in photovoltaic processes and the excited state dipole moment ( $\mu^*$ ) is the parameter that accounts for this phenomenon [10], thus the knowledge of  $\mu^*$  may be directly used to establish structure–property relationships related to the performance of OPV materials.

Among the experimental techniques to determine  $\mu^*$ , the solvatochromic methods have been extensively used due to their good compromise between facility, low cost and precision [11,12]. Solvatochromic models can be categorized into those considering specific solvent effects (hydrogen bond interactions) [13,14], and those considering nonspecifically the solvent effects, assuming instead that carefully selected probe molecules (generally dyes) with well-understood and strongly solvent-dependent spectral absorptions may serve as suitable models to be correlated with a variety of molecules under investigation. In this sense, a variety of empirical solvent polarity scales have been developed [15,16]. Particularly the  $E_T^N$  dimensionless scale of solvent polarity [17], based on the solvatochromism of pyridinium N-phenolate betaine

dyes, has been useful to correlate solvatochromism of Stokes shifts to estimate excited state dipole moments in a reliable way [18].

Taking as starting point our earlier theoretical study, herein we report the synthesis of novel push–pull dendrons, and the estimation of excited state dipole moments by the solvatochromic model involving the  $E_T^N$  polarity scale, in order to relate this parameter with the dendritic architecture and the potential performance of these organic compounds as photovoltaic candidates. Additionally the electron density distribution, by molecular orbitals and electrostatic potential maps, was used to rationalize the charge transfer processes on these branched molecules.

## Results and discussion

### Synthesis

Following the synthetic route shown in Fig. 1, fully conjugated dendrons (5) and (8) with donor–acceptor groups were obtained, as well as dendrons (6) and (9) with two different electron withdrawal groups,  $-\text{NO}_2$  and  $-\text{COH}$ , in the focal point and in the periphery respectively.

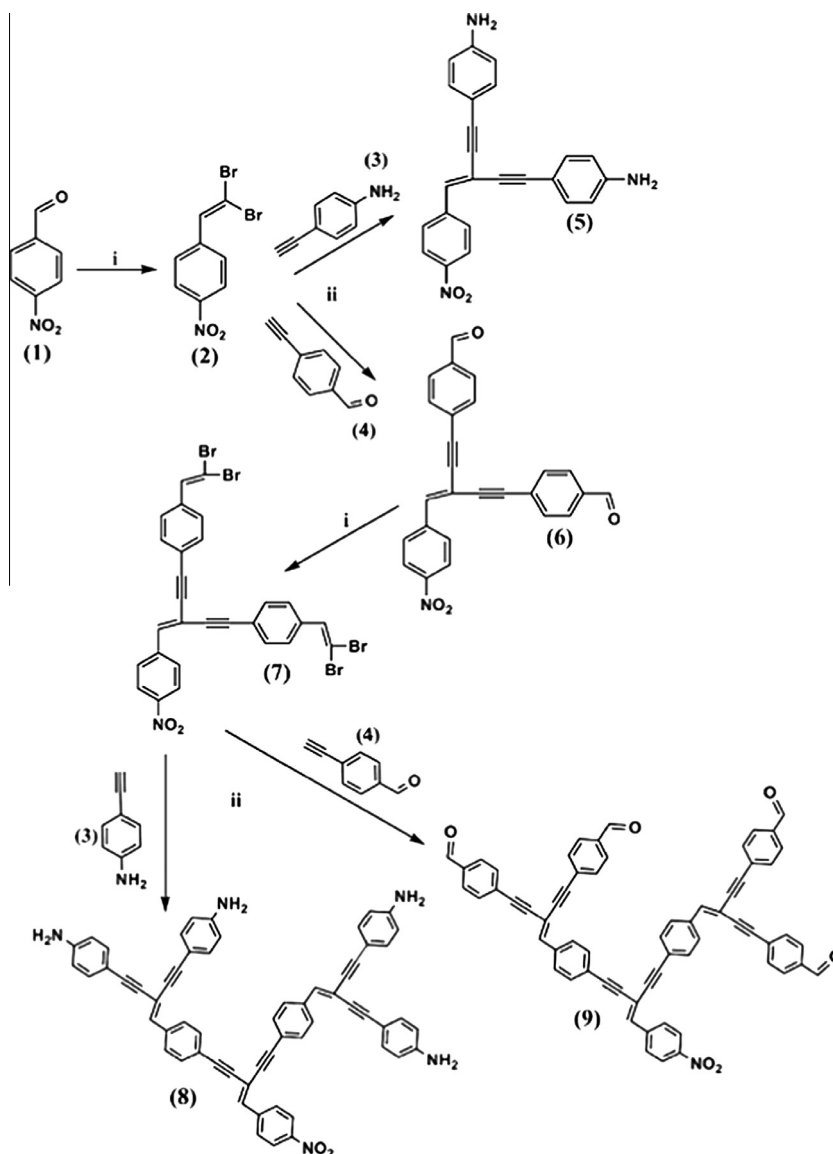


Fig. 1. Synthetic route to obtain fully conjugated dendrons. (i)  $\text{CBr}_4/\text{P}(\text{Ph})_3$ ,  $\text{CH}_2\text{Cl}_2$  (Wittig reaction); (ii)  $\text{Pd}(\text{OAc})_2/\text{NEt}_3$ , PEG-200 (C–C coupling reaction).

Iterative steps of activation and coupling were carried out iteratively by Wittig reaction and a modified protocol of classical palladium-catalyzed C–C coupling reaction [19] respectively. Polyethylene glycol-200 (PEG-200) was used as reaction medium in C–C coupling reactions.

A major problem of conventional C–C coupling reactions to obtain fully conjugated compounds is the loss of solubility when molecular weight increases [20]; therefore, mixtures of triethylamine/pyridine must be used in order to have homogeneous reaction media. The use of PEG-200 appears as an interesting option in terms of solubilization, and also as a reusable medium of reaction.

Considering the polarity balance in these molecules, the solubilization of reactants in PEG-200 to obtain the desired products was significantly improved; nevertheless subsequent chromatographic procedures were required to purify the target molecules. Additional acid-base selective extractions were carried out to obtain dendrons (5) and (9) with terminal –NH<sub>2</sub> groups.

Regarding the efficiency of the C–C coupling reaction in PEG-200, partial branched products were detected by NMR <sup>1</sup>H, attributable to a moderate performance of the palladium catalytic system in the reaction medium. A 1:1 ratio of mono- and di-substituted products of push-pull dendron (5) was found during the chromatographic purification, and characterized by NMR <sup>1</sup>H (Fig. 2).

The vinyl hydrogen labeled as 5 in the di-substituted product gets shifted toward lower fields when the substitution is incomplete (hydrogen 14 in the mono-substituted product), presumably due to the lack of the deshielding effect from the missing acetylenic group, and due to the presence of bromine. On the other hand, the electron withdrawal effect of the NO<sub>2</sub> group in the focal point of precursors should favor the coupling reaction, since the first step of the catalytic cycle involves an oxidative addition of palladium catalyst.

Bringing together the possible effects (including sterical hindrance), the result is the obtaining of the expected products in moderate yields.

All compounds (yellow-to-red solids with melting points up to 200 °C) were purified and verified by spectroscopic methods (FT-IR, NMR, UV–vis).

### UV–vis absorption–emission analysis

Absorption and emission spectra of dendrons (5), (8), (6) and (9) were measured in three different solvents (ethyl acetate, chloroform and methylene chloride) to subsequently estimate the excited state dipole moments ( $\mu^*$ ) by the solvatochromic method. Among the solvents commonly used in UV–vis spectroscopy, only few were able to dissolve the dendrons under study and that is why only three solvents were considered. The push–pull dendrons (5) and (8) were the main object of study, but also, for comparative purposes, we analyzed dendrons (6) and (9), with the electron withdrawal groups –NO<sub>2</sub> and –COH in the focal point and in the periphery respectively.

All dendrons exhibited similar patterns of absorption–emission as they share the same delocalized framework where the most likely electronic transitions should be  $\pi$ – $\pi^*$ . In Fig. 3 are shown the spectra of absorption and emission corresponding to push–pull dendron (8).

As expected, the emission spectra exhibit greater sensitivity to solvent polarity change, shifting the emission to lower energies due to the local stabilization of the polarized excited state by solvent molecules.

The marginal superposition between absorption and emission spectra observed in Fig. 3 suggests that the rigidity and high delocalization of these molecules promotes charge transfer mechanisms rather than resonant energy transfer ones (FRET) [21]. This is corroborated later by the analysis of molecular orbitals (Section ‘Theoretical analysis of electronic processes’). Also is interesting to analyze the profile of the emission spectra showing one regime of decay only, which can be related with practically one class of structural isomer, with the same distances and/or orientation between donor and acceptor groups, also related to the stiffness of the molecules.

Absorption and emission maxima for compounds (5), (8), (6) and (9) in three different solvents are shown in Table 1.

From Table 1, there is a bathochromic shift going from dendron (5) to (8) (first and second generations of push–pull dendrons respectively) corresponding to the extended conjugation, although

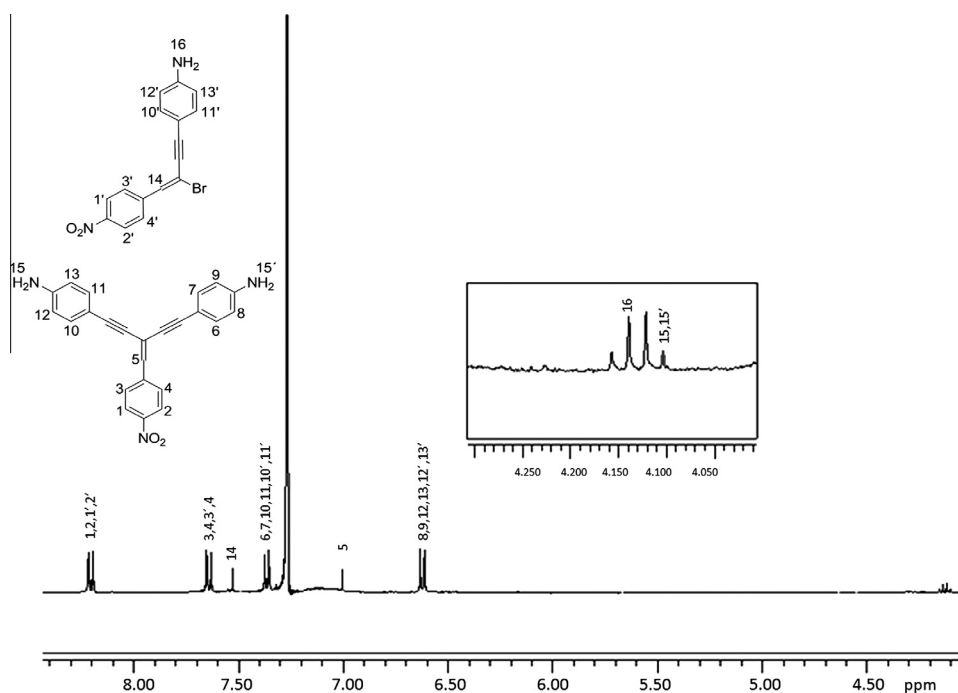


Fig. 2. <sup>1</sup>H NMR spectrum of mono- and di-substituted dendron (5), with one or two terminal –NH<sub>2</sub> groups.

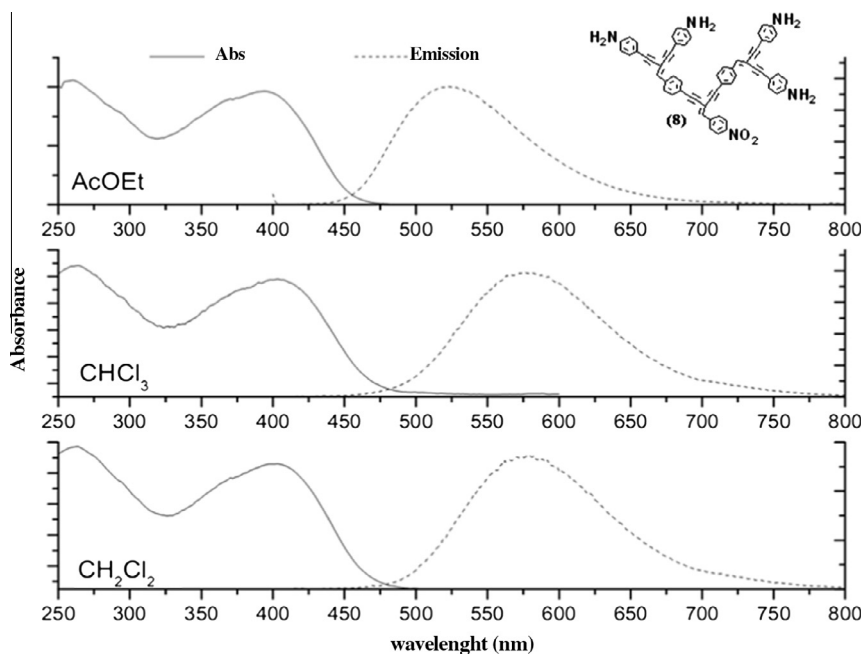


Fig. 3. Absorption and emission spectra (excitation at 350 nm) for dendron (8).

**Table 1**  
Absorption and emission maxima (nm).

Compound	Absorption maxima			Emission maxima <sup>a</sup>		
	AcOEt	CH <sub>2</sub> Cl <sub>2</sub>	CHCl <sub>3</sub>	AcOEt	CH <sub>2</sub> Cl <sub>2</sub>	CHCl <sub>3</sub>
(5)	350	376	371	514	547	550
(8)	396	407	406	523	578	569
(6)	375	387	387	462	490	494
(9)	358	372	366	519	550	541

<sup>a</sup> Excitation at 350 nm.

the steric hindrance. An opposite effect is observed going from first to second generation of dendrons with  $-\text{NO}_2$  and  $-\text{COH}$  groups in the focal point and in the periphery respectively. From theoretical calculations (see Section 'Theoretical analysis of electronic processes' below), conformational changes involved in the transition  $S_0 \rightarrow S_1$  for dendrons (8) and (9) were inspected (Fig. 4) and is observed that the excitation in case of dendron (9) does not result in a significant change in the structure, revealing the lack of the push–pull effect as driving force to electron delocalization throughout the molecule, and instead only the central conjugated fragment seems to participate during the excitation by its planari-

zation. Thus, an increment in steric hindrance appears to be the only effect when passing from first to second generation (dendrons (6) and (9)), causing the hypsochromic shift in the absorption maxima.

The analysis of solvent polarity effect (by dielectric constant;  $\epsilon$ ), on the Stokes shifts was carried out for the four dendrons under study. Solvents  $\text{CH}_2\text{Cl}_2$  and  $\text{CHCl}_3$ , with higher and lower  $\epsilon$  respectively, were considered in the analysis (see Table 2).

The larger Stokes shifts in  $\text{CH}_2\text{Cl}_2$  (solvent with higher dielectric constant) exhibited by push–pull dendrons (5) and (8), are related to an evident polarization in the excited state after charge separation processes, and the effect is more clear in case of dendron (8).

In contrast, lower Stokes shifts are related to dendrons (6) and (9) since no push–pull effect is present. Nonetheless, some degree of charge separation should occur as the excited states are yet sensitive to the polarity of the medium.

#### Dipole moments in excited state

Excited state dipole moments ( $\mu^*$ ) for dendrons (5), (8), (6) and (9) were estimated (Table 3) to relate this parameter with the efficiency of charge separation in these branched molecules.

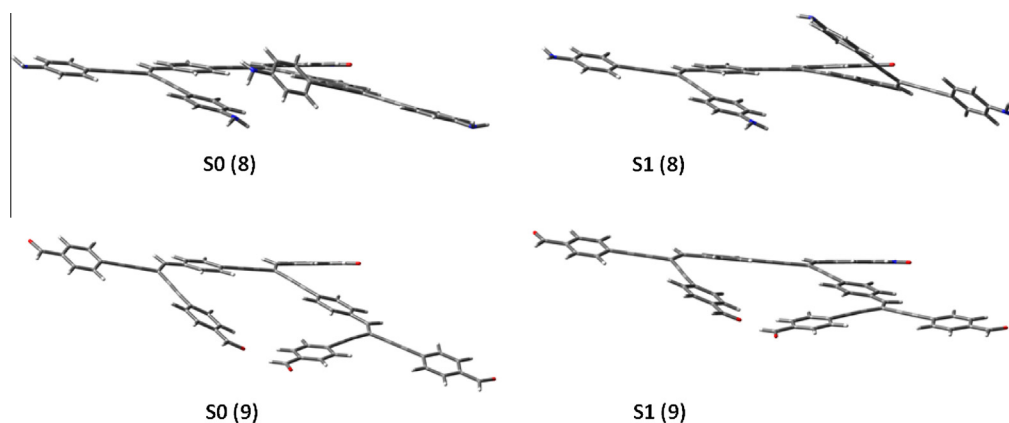


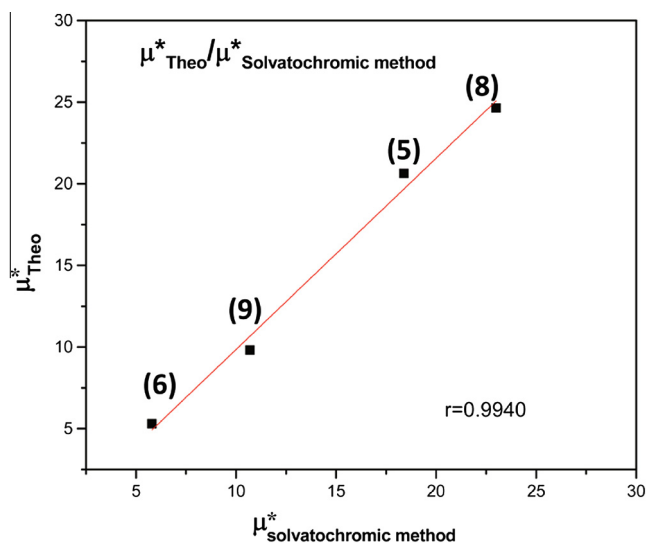
Fig. 4. Conformational changes involved in the transition  $S_0 \rightarrow S_1$  for dendrons (8) and (9) at TD-DFT M05-2X/cc-pVDZ level of theory.

**Table 2**  
Effect of the solvent dielectric constant ( $\epsilon$ ) on the Stokes shifts.

Molecule	Stokes shift (nm): CH <sub>2</sub> Cl <sub>2</sub> <sup>a</sup>	Stokes shift (nm): CHCl <sub>3</sub> <sup>b</sup>
(5)	179	171
(8)	224	208
(6)	107	103
(9)	175	178

<sup>a</sup>  $\epsilon = 8.93$ .<sup>b</sup>  $\epsilon = 4.81$ .**Table 3**  
Excited state dipole moments estimated by both, solvatochromic method ( $\mu^*$ ) and TD-DFT M05-2X/cc-pVDZ ( $\mu_{\text{Theo}}^*$ ).

Dendron	$\mu_0^a$ (Debyes)	$\mu^*$ (Debyes)	$\mu_{\text{Theo}}^*$ (Debyes)
(5)	10.6	18.4	20.63
(8)	14.8	22.3	24.64
(6)	1.4	5.8	5.3
(9)	4.8	10.7	9.81

<sup>a</sup> Theoretical dipole moments in ground state (level of theory: M05-2X/cc-pVDZ) in chloroform.**Fig. 5.** Correlation between  $\mu^*$  (by solvatochromic method) and  $\mu_{\text{Theo}}^*$  (by TD-DFT M05-2X/cc-pVDZ) estimated in Debye (D) for all dendrons under study.

According to the formulation of the solvatochromic model (see Supporting information), the  $\mu^*$  values were achieved from the slope of the graph of Stokes shifts versus  $E_T^N$  values of the solvents used (chloroform and methylene chloride), involving also parameters such as ground state dipole moments ( $\mu_0$ , shown in Table 3) and Onsager radii ( $a_0$ ), theoretically calculated in chloroform (M05-2X/cc-pVDZ level of theory).

For comparative and validation purposes, the excited state dipole moments of the dendrons under study were fully theoretically calculated (TD-DFTM05-2X/cc-pVDZ level of theory) and the results labeled as  $\mu_{\text{Theo}}^*$  are also shown in Table 3.

The charge transfer degree on photoexcitation can be estimated by the comparison of the dipole moments in ground and excited state. Higher values of  $\mu^*$  exhibited by the push-pull dendrons (5) and (8), as well as higher deltas between dipole moments in ground and excited state can be related to an efficient charge separation in excited state, resulting in a zwitterionic structures,

**Table 4**  
Molecular orbitals involved in S0  $\rightarrow$  S1 transition and the corresponding expansion coefficients (Cj).

Molecule	S0 $\rightarrow$ S1	Cj
(5)	HOMO-2 $\rightarrow$ LUMO	0.14914
	HOMO $\rightarrow$ LUMO	0.67236
(6)	HOMO $\rightarrow$ LUMO	0.68581
	HOMO-4 $\rightarrow$ LUMO	0.25222
(8)	HOMO-1 $\rightarrow$ LUMO+1	0.24994
	HOMO $\rightarrow$ LUMO	0.57105
	HOMO $\rightarrow$ LUMO+2	-0.12277
	HOMO-2 $\rightarrow$ LUMO	0.12937
	HOMO-2 $\rightarrow$ LUMO+2	-0.14489
(9)	HOMO-1 $\rightarrow$ LUMO+1	0.26992
	HOMO $\rightarrow$ LUMO	0.60427

imposed by charge transfer interactions between donor and acceptor groups (see Ref. [9]). Organic materials with dipole moments even lower (around 10 Debye) are seriously considered as sensitizers for dye-sensitized solar cells [22,23]. Consistent with the nature of dendrons (6) and (9), the dipole moments are lower, both in the ground and excited state.

As shown in Fig. 5, there is a very good correlation between  $\mu^*$  and  $\mu_{\text{Theo}}^*$  values, which validates the theoretical method.

#### Theoretical analysis of electronic processes

Molecular orbitals involved in the transition S0  $\rightarrow$  S1 were calculated and the corresponding expansion coefficients (Cj) are shown in Table 4 for dendrons (5), (6), (8) and (9). In all cases the most important contribution to S0  $\rightarrow$  S1 transition is the HOMO-LUMO excitation.

Molecular orbitals (MO) contributing to the excitation are shown in Fig. 6. In case of dendrons (6) and (9) with -NO<sub>2</sub> and -COH groups, the electron density is mainly distributed on central conjugated fragments, with a consistent contribution from -NO<sub>2</sub> to the LUMO. Although the electron density extends from HOMO-2 to LUMO+2 orbitals in case of Dendron (9), there is an ambiguous distribution between terminal groups since the push-pull effect is absent.

On the other hand, the push-pull effect in case of dendrons (5) and (8) is evidenced by unambiguous contributions of -NH<sub>2</sub> and -NO<sub>2</sub> groups to HOMO and LUMO orbitals respectively.

From the MO representation of push-pull dendron (8) is observed an equivalent branched electron distribution between HOO-1 and HOMO, and when the orbital energies are analyzed is found that these two molecular orbitals are virtually degenerate with energies of -0.2329 and -0.2307 hartrees respectively. Such orbital partitioning suggests a collective contribution of resonant structures that enhance the charge separation through the branched architecture, in contrast to that expected in linear molecules.

The charge separation during the excitation can be visualized in Fig. 7 via the dipole moments. Here, the molecular electrostatic potential for dendrons (8) and (9) was mapped onto the electronic density for the S0 and S1 states.

From Fig. 7 is observed that charge separation is greater in the excited state than in the ground state for dendron (8) and the distribution of the negative electrostatic potential extends throughout the entire molecular framework. In case of dendron (9) there are not evident changes between S0 and S1 states. From this representation is illustrated again the collective branched contribution to the charge separation in excited state when the push-pull scenario is present.

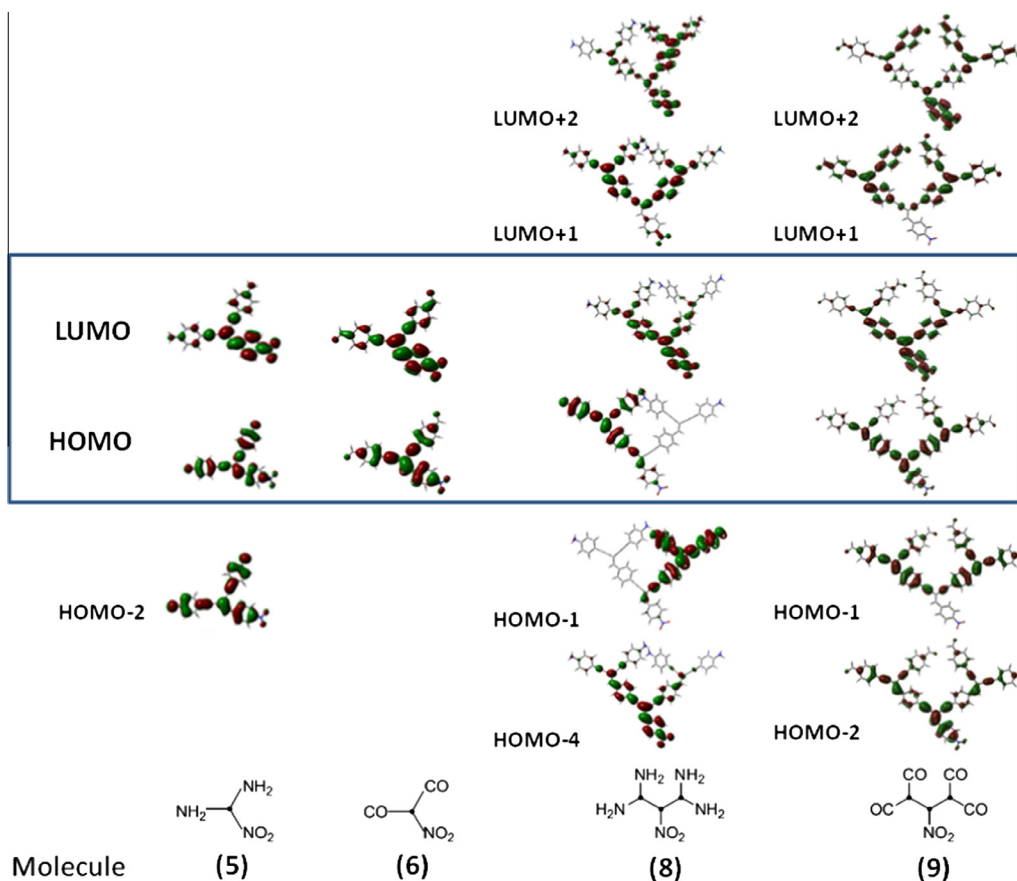


Fig. 6. Molecular orbitals involved in  $S_0 \rightarrow S_1$  transition for (5), (6), (8) and (9).

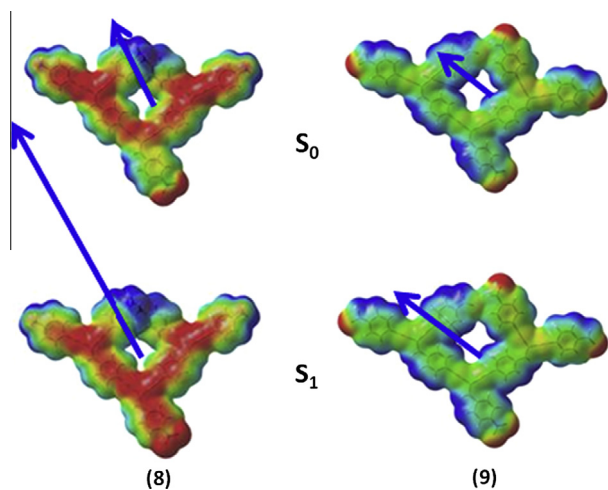


Fig. 7. Molecular electrostatic potential mapped onto electron density for dendrons (8) and (9). Red color represents negative values and blue color represents positive values. Dipole moment vector is displayed. (For interpretation of the references to colour in this figure legend, the reader is referred to the web version of this article.)

## Conclusions

The synthesis of novel push–pull dendrons, following a modified protocol to conventional C–C coupling reaction as a suitable method, was described. From the UV–vis absorption–emission analysis, the dendritic compounds appear as rigid and highly delocalized systems, according to their spectral features.

The effect of the polarity of the solvent was more evident in case of dendrons (5) and (8) with donor–acceptor groups. Larger

Stokes shifts related to better solvation of the excited state were observed in presence of the solvent with higher dielectric constant ( $\text{CH}_2\text{Cl}_2$ ).

The solvatochromic model based on the  $E_T^N$  dimensionless scale of solvent polarity appears as an accessible tool to estimate dipole moments in the excited state. The results obtained by this model are in a good agreement with theoretical calculations of dipole moments in the excited state, which validates the theoretical method.

The dendron (8) exhibited the largest dipole moment in both ground and excited state, due to an efficient electronic delocalization from one end to the other of the molecule, through the  $\pi$  framework and, comparing push–pull dendrons (5) and (8), the charge separation is more effective as the dendritic generation increases.

The MO representation of push–pull dendron (8) shown an equivalent branched electron distribution between HOMO–1 and HOMO (virtually degenerated) which promotes a collective contribution of resonant structures, desirable to an efficient charge separation, as is corroborated by the molecular electrostatic potential maps.

Considering that the dissociation of excitons into free charge carriers is crucial in photovoltaic processes, the dendritic donor–acceptor frameworks (dendrons 5 and 8) having exhibited the highest values of excited state dipole moments can be promising as organic photovoltaics.

## Experimental section

### Materials and methods

Monomers 4-nitrobenzaldehyde, 4-ethynylaniline, and precursor 4-bromobenzaldehyde were used as received. Except

methylene chloride (freshly distilled before use), solvents and reagents were used without further purification. NMR (CDCl<sub>3</sub>) and FT-IR spectra were recorded in spectrometer Bruker Avance 400 MHz, and FT-IR Nicolette Model PCIR, respectively.

The visible absorption and emission (excitation at 350 nm) spectra were measured by Double Beam, UNICAM spectrometer and Cary-Eclipse Varian fluorescence spectrometer respectively. Solutions of  $1 \times 10^4$  µg/L were prepared in three different solvents: methylene chloride, ethyl acetate and chloroform, and measured in the absorbance range of Lambert–Beer law.

#### Estimation of dipole moments in excited state ( $\mu^*$ ) by solvatochromic methods

The excited state dipole moments of synthesized molecules were estimated by the solvatochromic method, according to Koutek formulation [24], using the solvent parameter  $E_T^N$  for methylene chloride and chloroform (0.309 and 0.259 respectively). Parameters like dipole moments and Onsager radii in ground state, involved in the mathematical model [25,26], were obtained from theoretical calculations for the molecules under study. A detailed description of the method can be found in [Supporting information](#).

#### Computational details

Theoretical calculations were carried out using Gaussian 09 suite of programs [27]. The selected model was M05-2X [28] in combination with the basis set cc-pVDZ [29]. The validation of the method is described in [Supporting information](#).

For each molecule under study, a structural optimization for the ground state (S0) was carried out, and afterwards the optimized structure was used for the calculation of the excitation (S1) by time dependent density functional theory (TD-DFT) model.

All the calculations (single points and structural optimizations either in ground and excited states) were carried out in three different solvents: methylene chloride, chloroform and ethyl acetate, using the PCM model [30] incorporated in Gaussian 09 suite of programs.

#### Synthesis

All synthetic details can be found in [Supporting information](#); here is shown the summary of spectroscopic characterization.

$\beta,\beta$ -dibromo-4-nitrostyrene (2). Yellow solid (m.p. 50–52 °C) in 65% yield.

<sup>1</sup>H NMR (CDCl<sub>3</sub>): 8.20 (d, 2H, *ortho* to NO<sub>2</sub>), 7.70 (d, 2H *meta* to NO<sub>2</sub>), 7.45 (HC=C). FT-IR (cm<sup>-1</sup>): 3056 (CH arom.), 1590 (C=C arom.), 1189 y 1120 (C–N), 696 (C–Br), 1484 (N–O).

4-ethynylbenzaldehyde (4). Yellow solid (m.p. 64–65 °C) in 80% yield.

<sup>1</sup>H NMR (CDCl<sub>3</sub>): 3.30 (s, 1H HC=C), 7.80 (d, 2H arom.), 7.60 (d, 2H arom.), 10.02 (s, 1H, CHO). FT-IR (cm<sup>-1</sup>): 2890 (C–H arom.), 2150 (C=C), 1700 (C=O), 1600 (C=C arom.).

$\beta,\beta$ -di(4'-aminophenylethynyl)-4-nitrostyrene (5). Dark orange solid (m.p. 140–142 °C) in 51% yield.

<sup>1</sup>H NMR (CDCl<sub>3</sub>): 8.2 (d, 2H, *ortho* to NO<sub>2</sub>), 7.6 (d, 2H, *meta* to NO<sub>2</sub>), 7.5 (s, 1H, HC=C), 7.3 (d, 2H, *meta* to NH<sub>2</sub>), 6.6 (d, 2H, *ortho* to NH<sub>2</sub>). FT-IR (cm<sup>-1</sup>): 2864 (CH), 3430 (NH), 2357–1946 (C=C), 1600 (C=C arom.), 1454 (N–O).

$\beta,\beta$ -(4'-formylphenylethynyl)-4-nitrostyrene (6). Brown-orange solid (m.p. 150–152 °C) in 53% yield.

<sup>1</sup>H NMR (CDCl<sub>3</sub>): 10.06 (s, 2H CHO), 8.28 (d, 2H, *ortho* to NO<sub>2</sub>), 7.89 (d, 4H *meta* CO), 7.71 (d, 4H *ortho* to CO), 7.53 (s, 1H, HC=C); FT-IR (cm<sup>-1</sup>): 3061 (CH arom.), 2920 (CH aliph.), 2207 (C=C), 1695 (C=O), 1426 (NO<sub>2</sub>), 1596 (C=C arom.).

$\beta,\beta$ -Bis( $\beta,\beta'$ -dibromostyryl-4'-ethynyl)-4-nitrostyrene (7). Reddish solid (m.p. 85–87 °C) in 45% yield.

<sup>1</sup>H NMR (CDCl<sub>3</sub>): 8.25 (d, 2H, *ortho* to NO<sub>2</sub>), 8.07 (d, 2H, *meta* to NO<sub>2</sub>), 7.71 (dd, 4H, *meta* to dibromostyryl), 7.56 (dd, 4H, *ortho* to dibromostyryl), 7.53 (s, 2H, HC=CBr<sub>2</sub>). FT-IR (cm<sup>-1</sup>): 3056 (C–H arom.), 2200 (C=C), 1600 (C=C arom.), 1484 (NO<sub>2</sub>), 1185 and 1120 (C–N), 696 (C–Br).

Bis[ $\beta,\beta$ -di( $\beta,\beta'$ -dianilinephenylethynyl-4-styryl-4'-ethynyl)-4-styryl] nitrostyrene (8). Reddish solid (m.p. 189–192 °C) in 30% yield.

<sup>1</sup>H NMR (CDCl<sub>3</sub>): 8.35 (d, 2H, *ortho* to NO<sub>2</sub>), 8.08 (d, 2H, *meta* to NO<sub>2</sub>), 7.95 (dd, 4H, *ortho* to 4'-ethynyl), 7.52 (dd, 4H, *meta* to 4'-ethynyl), 7.64 (m, 8H, *meta* to NH<sub>2</sub>), 7.49 (m, 8H, *ortho* to NH<sub>2</sub>), 7.12 (s, 1H, HC=C), 7.13 (s, 1H, HC=C), 7.00 (s, 1H, HC=C), 3.95 (8H, NH<sub>2</sub>). FT-IR (cm<sup>-1</sup>): 3402 (N–H), overtones > 3402 (N–H), 2865 (C–H), 2367 (C=C), 1643 (C=C arom.), 1452 (NO<sub>2</sub>), 1348 (NO<sub>2</sub>), 883, 834 (*para*-substitution).

Bis[ $\beta,\beta$ -di( $\beta,\beta'$ -diformylphenylethynyl-4-styryl-4'-ethynyl)-4-styryl] nitrostyrene (9). Reddish solid (m.p. 202–204 °C) in 30% yield.

<sup>1</sup>H NMR (CDCl<sub>3</sub>): 10.10 (4dd, 4H, HCO), 8.40 (d, 2H, *ortho* to NO<sub>2</sub>), 8.08 (dd, 2H, *meta* to NO<sub>2</sub>), 7.83 (dd, 4H, *ortho* to 4'-ethynyl), 7.54 (dd, 4H, *meta* to 4'-ethynyl), 7.68 (m, 8H, *meta* to formyl), 7.48 (m, 8H, *ortho* to formyl), 7.00 (s, 3H, HC=C). FT-IR (cm<sup>-1</sup>): 3020 (CH arom.), 2200 (C=C), 1695 (C=O), 1590 (C=C), 1510 (NO<sub>2</sub> arom.), 1320 (NO<sub>2</sub>).

#### Acknowledgements

We are grateful to PAPIIT IN-101512/24 and IB101712 for financial support. The authors wish to thanks A. Peña-Huerta and G. Cedillo-Valverde for NMR study, and Joaquín Morales and Caín González for technical support.

#### Appendix A. Supplementary material

Supplementary data associated with this article can be found, in the online version, at <http://dx.doi.org/10.1016/j.molstruc.2014.12.043>.

#### References

- [1] J.L. Bredas, J.E. Norton, J. Cornil, V. Coropceanu, *Acc. Chem. Res.* 42 (2009) 1691.
- [2] A. Mishra, P. Bäuerle, *Angew. Chem. Int. Ed.* 51 (2012) 2020.
- [3] Ch. Li, M. Liu, N.G. Pschirer, M. Baumgarten, K. Müllen, *Chem. Rev.* 110 (2010) 6817.
- [4] S.Ch. Lo, P.L. Burn, *Chem. Rev.* 107 (2007) 1097.
- [5] W.J. Mitchell, N. Kopidakis, G. Rumbles, D.S. Ginley, S.E. Shaheen, *J. Mater. Chem.* 15 (2005) 4518.
- [6] J.L. Segura, F. Giacalone, R. Gómez, N. Martín, D.M. Guldi, Ch. Luo, A. Swartz, I. Riedel, D. Chirvase, J. Parisi, V. Dyakonov, N.S. Sariciftci, F. Padinger, *Mater. Sci. Eng. C* 25 (2005) 835.
- [7] C.C. Kwok, M.S. Wong, *Macromolecules* 34 (2001) 6821.
- [8] J. Sun, L. Wang, X. Yu, X. Zhang, *Eur. Polym. J.* 41 (2005) 1219.
- [9] E. Ramos, P. Guadarrama, G. Terán, S. Fomine, *J. Phys. Org. Chem.* 22 (2009) 9.
- [10] B. Carsten, J.M. Szarko, H.J. Son, W. Wang, L. Lu, F. He, B.S. Rolczynski, S.J. Lou, L.X. Chen, L. Yu, *J. Am. Chem. Soc.* 133 (2011) 20468.
- [11] U.S. Raikar, V.B. Tangod, S.R. Mannopantar, B.M. Mastiholi, *Opt. Commun.* 283 (2010) 4289.
- [12] X. Liu, J.M. Cole, K.S. Low, *J. Phys. Chem. C* 117 (2013) 14731.
- [13] M.J. Kamlet, R.W. Taft, *J. Am. Chem. Soc.* 98 (1976) 377.
- [14] R.W. Taft, M.J. Kamlet, *J. Am. Chem. Soc.* 98 (1976) 2886.
- [15] C. Reichardt, *Chem. Rev.* 94 (1994) 2319.
- [16] W.R. Fawcett, *J. Phys. Chem.* 97 (1993) 9540.
- [17] C. Reichardt, E. Harbusch-Gornert, *Liebigs Ann. Chem.* (1983) 721.
- [18] M. Ravi, A. Samanta, T.P. Radhakrishnan, *J. Phys. Chem.* 98 (1994) 9133.
- [19] S. Chandrasekhar, Ch. Narsihmulu, S.S. Sultana, N.R. Reddy, *Org. Lett.* 4 (2002) 4399.
- [20] L. Fomina, P. Guadarrama, S. Fomine, R. Salcedo, T. Ogawa, *Polymer* 39 (1998) 2629.
- [21] G. Bongiovanni, C. Botta, J.E. Communal, F. Cordella, L. Magistrelli, A. Mura, G. Patrinoiu, P. Picouet, G. Di-Silvestro, *Mater. Sci. Eng. C* 23 (2003) 909.
- [22] C. Li, M. Liu, N.G. Pschirer, M. Baumgarten, *Chem. Rev.* 110 (2010) 6817.

- [23] Ch. Jiao, K.W. Huang, Ch. Chi, J. Wu, *J. Org. Chem.* **76** (2011) 661.
- [24] B. Koutek, *Chem. Commun.* **43** (1978) 2368.
- [25] S. Kumar, S.K. Jain, R.C. Rastogi, *Spectrochim. Acta Part A* **57** (2001) 291.
- [26] S. Kumar, V.C. Rao, R.C. Rastogi, *Spectrochim. Acta Part A* **57** (2001) 41.
- [27] M.J. Frisch, G.W. Trucks, H.B. Schlegel, G.E. Scuseria, M.A. Robb, J.R. Cheeseman, G. Scalmani, V. Barone, B. Mennucci, G.A. Petersson, H. Nakatsuji, M. Caricato, X. Li, H.P. Hratchian, A.F. Izmaylov, J. Bloino, G. Zheng, J.L. Sonnenberg, M. Hada, M. Ehara, K. Toyota, R. Fukuda, J. Hasegawa, M. Ishida, T. Nakajima, Y. Honda, O. Kitao, H. Nakai, T. Vreven, J.A. Montgomery, Jr., J. E. Peralta, F. Ogliaro, M. Bearpark, J.J. Heyd, E. Brothers, K.N. Kudin, V.N. Staroverov, R. Kobayashi, J. Normand, K. Raghavachari, A. Rendell, J.C. Burant, S.S. Iyengar, J. Tomasi, M. Cossi, N. Rega, J.M. Millam, M. Klene, J.E. Knox, J.B. Cross, V. Bakken, C. Adamo, J. Jaramillo, R. Gomperts, R.E. Stratmann, O. Yazyev, A.J. Austin, R. Cammi, C. Pomelli, J.W. Ochterski, R.L. Martin, K. Morokuma, V.G. Zakrzewski, G.A. Voth, P. Salvador, J.J. Dannenberg, S. Dapprich, A.D. Daniels, Ö. Farkas, J.B. Foresman, J.V. Ortiz, J. Cioslowski, D.J. Fox, Gaussian 09, Revision A.1, Gaussian Inc., Wallingford CT, 2009.
- [28] Y. Zhao, N.E. Schultz, D.G. Truhlar, *J. Chem. Theory Comput.* **2** (2006) 364.
- [29] T.H. Dunning Jr., *J. Chem. Phys.* **9** (1989) 1007.
- [30] J. Tomasi, B. Mennucci, R. Cammi, *Chem. Rev.* **105** (2005) 2999.